

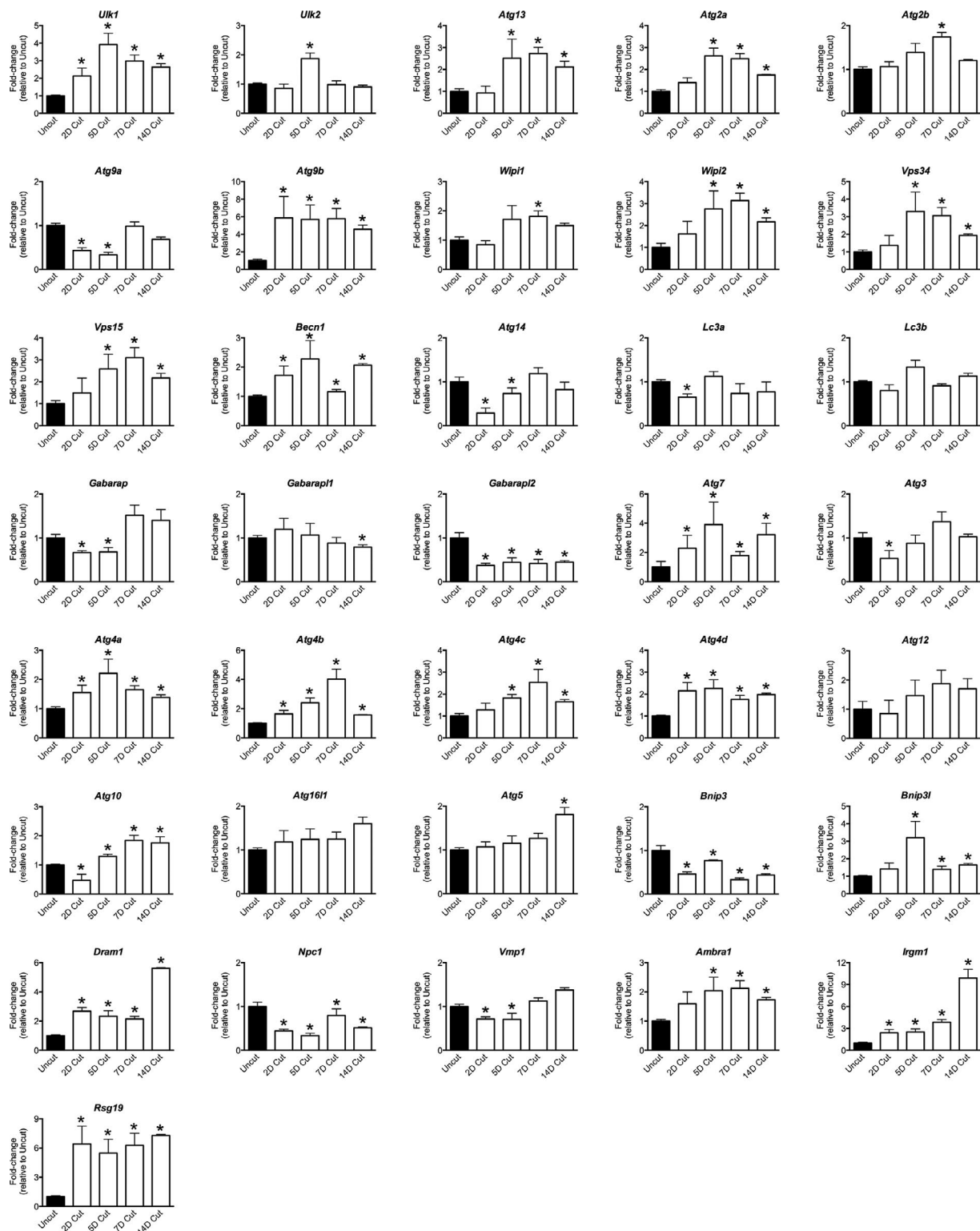
Gomez-Sanchez et al., <http://www.jcb.org/cgi/content/full/jcb.201503019/DC1>

Figure S1. **qPCR analysis of autophagy-related genes.** Bar graphs depicting changes in expression of autophagy-related genes after nerve injury, as shown in Fig. 1 A. $n = 3$ mice for each time point. Data are presented as mean \pm SEM (error bars). *, $P < 0.05$.

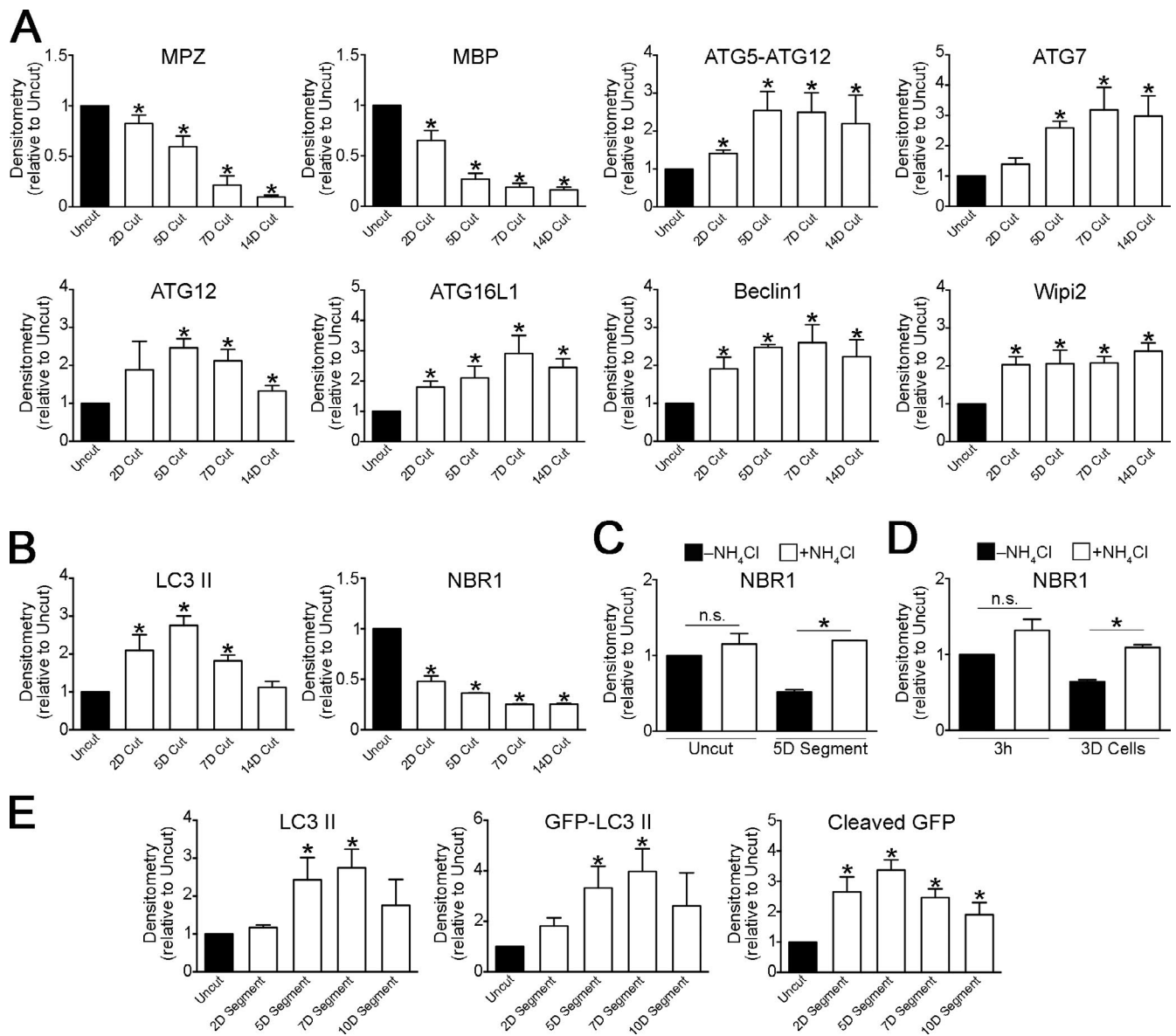


Figure S2. **Western blot quantification.** (A) Densitometric quantification of Western blots from Fig. 1 B. For each comparison, the value for cut nerves is normalized to that seen in uncut nerves. (B) Densitometric quantification of Western blots from Fig. 1 C. For each comparison, the value for cut nerves is normalized to that seen in uncut nerves. (C) Densitometric quantification of NBR1 Western blots from Fig. 1 D. For each comparison, the values for different conditions are normalized to those seen in uncut nerves without NH₄Cl treatment. (D) Densitometric quantification of NBR1 Western blots from Fig. 1 E. For each comparison, the values for different conditions are normalized to those seen in freshly plated Schwann cell cultures without NH₄Cl treatment. (E) Densitometric quantification of Western blots from Fig. 1 F. For each comparison, the value for nerve segments maintained in vitro for different time points is normalized to that seen in uncut nerves. Data are presented as mean ± SEM (error bars) from three independent experiments. *, P < 0.05; n.s., not significant.

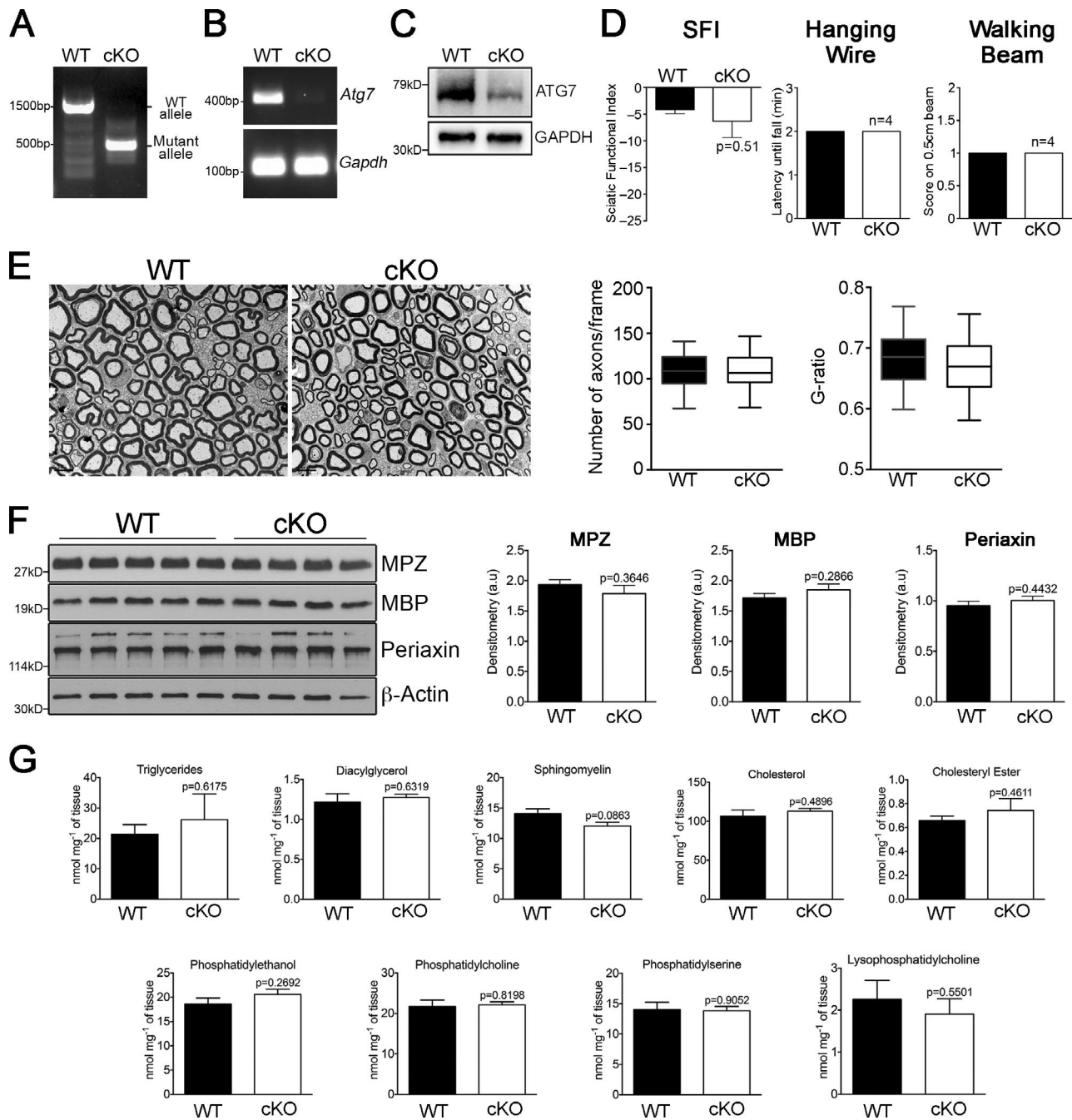


Figure S3. Uninjured *Atg7* cKO nerves are normal. (A) RT-PCR showing the mutant allele in genomic DNA samples from P8 purified Schwann cells from *Atg7* cKO mice. (B) RT-PCR showing reduced expression of *Atg7* mRNA in P8 purified Schwann cells from *Atg7* cKO mice. (C) Western blot showing reduced expression of ATG7 in P8 Schwann cells (~95% pure) from *Atg7* cKO mice. The residual ATG7 band that remains is likely due to the presence of contamination with fibroblasts (~5% of total cell population). (D) Behavioral analyses (sciatic function index [SFI], hanging wire, and walking beam) show that P90 *Atg7* cKO mice fed ad libitum have normal sensorimotor function. Sciatic function index: *Atg7* cKO mice and control mouse paws were analyzed for toe spreading and footprint length, and used to calculate SFI values. *Atg7* cKO mice and control mice were within a healthy range of SFI values and were not found to be significantly different. Hanging wire: *Atg7* cKO and control mice were allowed to hang upside-down from a grid for 2.0 min to assess grip strength. *Atg7* cKO mice and control mice all remained on the grid for the full length of time and were not found to be significantly different. Walking beam: *Atg7* cKO and control mice were allowed to walk across a 0.5-cm beam and were scored on foot slips and falls (higher score = worse performance). *Atg7* cKO mice and control mice all scored in the lowest range and performed as expected for healthy mice. $n = 4$ mice for each genotype. Data are presented as mean \pm SEM (error bars). Individual p-values are shown. (E) Electron micrographs showing normal myelin profile in uncut nerves from P90 *Atg7* cKO mice fed ad libitum. Box plots show quantification of axonal numbers (left) and G ratio (right) in control and *Atg7* cKO sciatic nerves. $n = 3$ mice for each genotype. Box plots correspond to center quartiles, with the black bar indicating the median, and whiskers extend from the 5th to the 95th percentiles. (F) Western blot analysis showing normal levels of myelin proteins MPZ, MBP, and periaxin in uncut nerves from P90 control and *Atg7* cKO mice fed ad libitum. Graphs show densitometric analyses of these myelin proteins (relative to *Gapdh*). $n =$ a minimum of four mice for each genotype. Data are presented as mean \pm SEM (error bars); individual p-values are shown. (G) Thin-layer chromatography analysis shows no significant differences in the amount of different lipid classes in control and *Atg7* cKO mice. $n =$ a minimum of 4 mice for each genotype. Data are presented as mean \pm SEM (error bars); individual p-values are shown.

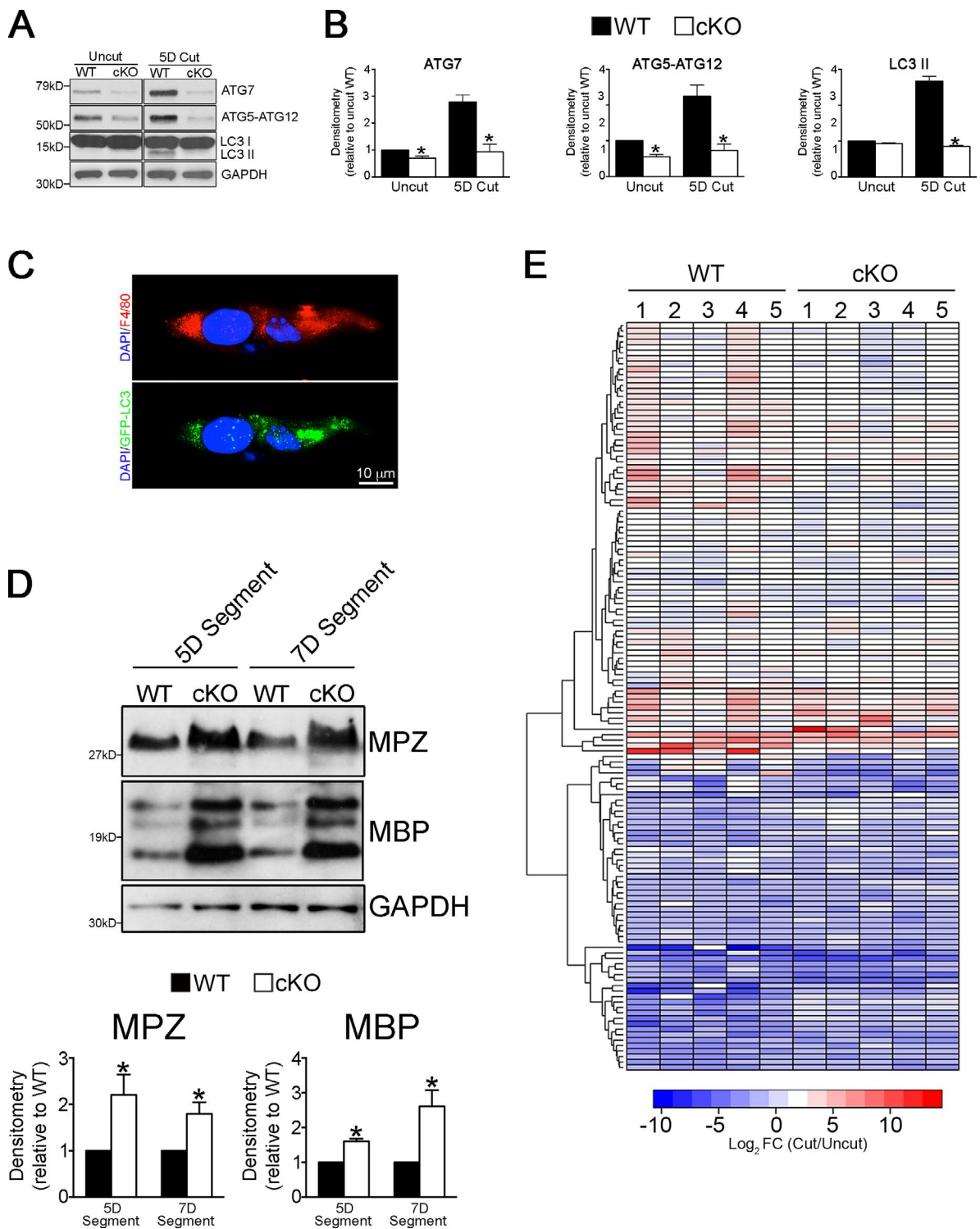


Figure S4. **Genetic inactivation of autophagy retards myelin degradation.** (A) Western blot showing reduced levels of ATG7 and ATG5-ATG12 in uncut and 5 d cut nerves from Atg7 cKO mice, compared with WT nerves. In addition, the increase in LC3 II levels seen after nerve cut in WT nerves compared with uncut nerves is not seen after nerve transection in Atg7 cKO mice. Please note that Atg7 cKO nerves have residual expression of ATG7 and ATG5-ATG12, which is likely due to the presence of contaminating cells in the nerves, including endoneurial and perineurial fibroblasts, and resident macrophages, which also activate autophagy (C). (B) Densitometric quantification of Western blots shows significantly lower levels of ATG7, ATG5-ATG12, and LC3 II in uncut and 5 d cut nerves from Atg7 cKO mice, compared with WT nerves. Data are presented as mean \pm SEM (error bars) from three independent experiments. *, $P < 0.05$ (Atg7 cKO relative to WT). (C) Immunolabeling showing expression of GFP-LC3 puncta in F4/80⁺ macrophages found in 5 d cut nerves. (D) Western blot analysis showing reduced degradation of the myelin proteins MPZ and MBP from Atg7 cKO nerve segments maintained in vitro for 5 and 7 d. Densitometric analysis of Western blots showing higher levels of myelin proteins in nerve segments from Atg7 cKO mice compared with WT controls. For each comparison, the value for cKO is normalized to that seen in WT. Data are presented as mean \pm SEM (error bars) from three independent experiments. *, $P < 0.05$ (Atg7 cKO relative to WT). (E) Heat map showing proteomics analysis of 5 d cut nerves from control and Atg7 cKO mice. Data are expressed as log₂ fold change of cut nerves relative to control uninjured nerves (red-blue color scale) for each of five replicates (1–5) for each genotype.

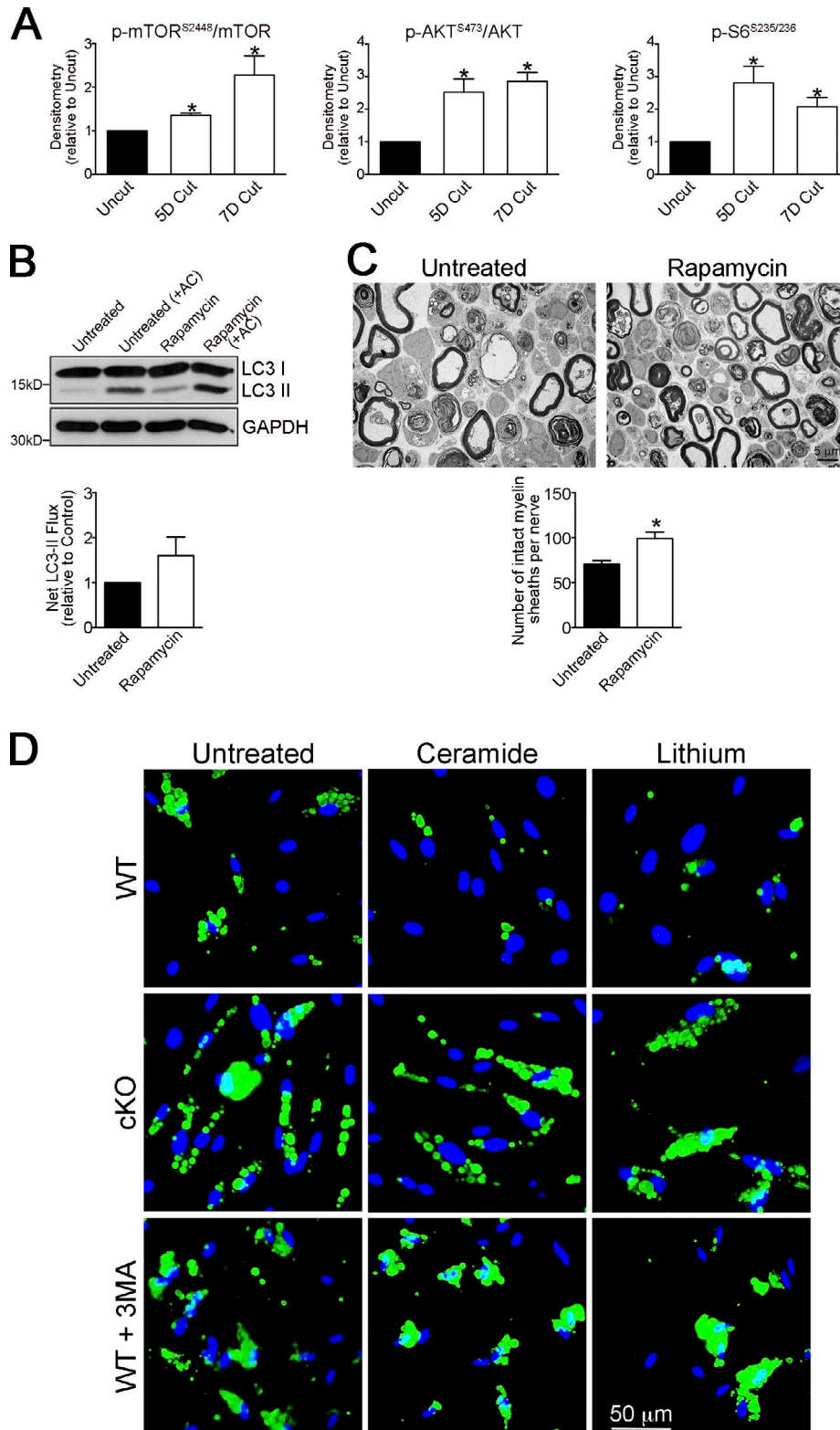


Figure S5. **Regulation of myelinophagy.** (A) Densitometric quantification of Western blots from Fig. 6 A. For each comparison, the value for cut nerves is normalized to that seen in uncut nerves. Data are presented as mean \pm SEM (error bars) from three independent experiments. *, $P < 0.05$ (cut nerves relative to uncut nerves). (B) Western blot showing increased LC3 II accumulation in nerve segments maintained in vitro for 5 d in the presence of NH_4Cl (3 h treatment). The graph shows no significant difference in net LC3 II flux after rapamycin treatment compared with control cultures. Data are presented as mean \pm SEM (error bars) from three independent experiments. (C) Electron micrographs showing similar numbers of intact myelin sheaths in nerve segments cultured in vitro for 3 d in the presence of rapamycin, compared with control cultures. The graph shows quantification of the number of intact myelin sheaths in control segments and segments treated with rapamycin. Data are presented as mean \pm SEM (error bars) from three independent experiments with a minimum of picture frames analyzed per condition/experiment. *, $P < 0.05$. (D) Immunolabeling showing regulation of MPZ breakdown by ceramide or lithium in dissociated Schwann cell cultures from P8 WT or *Atg7* cKO mice, treated 3 d in vitro.

Table S1. List of primers used for RT-qPCR

Gene		Accession	Sense sequence (5'-3')	Antisense sequence (5'-3')
<i>Ulk1</i>	unc-51 like kinase 1	NM_009469.3	TGCGCATAGTGTGCAGGTAG	AACATCGTGGCGCTGTATGA
<i>Ulk2</i>	unc-51 like kinase 2	NM_013881.4	CCTTTAGGTGGACACCCAGGG	GGCAATGCCAGCATAACACC
<i>Atg13</i>	Autophagy related 13	NM_145528.3	TTCCACATCCCCCTCCCTCC	AGAAGGCATGTGCATCACCA
<i>Atg2a</i>	Autophagy related 2A	NM_194348.3	ATCCGTAAGAACCAGCTGCC	GCGCCCATCTTCTGTACT
<i>Atg2b</i>	Autophagy related 2B	NM_029654.4	CGTGTGTTCAACTGCACCAG	GCGATCTCCGGTAACTTCT
<i>Atg9a</i>	Autophagy related 9A	NM_001003917.4	CGAGGGGAGCAAATCACCTT	TGAAGGCAACCACAAAGAGGA
<i>Atg9b</i>	Autophagy related 9B	NM_001002897.3	GGTGTTTTACAGGGAGGCC	CTCTGCAGTCCAGGAGGC
<i>Wipi1</i>	WD repeat domain, phosphoinositide interacting 1	NM_145940.2		
			CACAGGACGCCTGAACTTCT	GTAAGGTGTCCGTCGGAGG
<i>Wipi2</i>	WD repeat domain, phosphoinositide interacting 2	NM_178398.4		
			GCTGTTGGTAGTAAGTCCGGG	GCTTTGAGGCTGACAATGGC
<i>Vps34</i>	Phosphoinositide-3-kinase, class 3	NM_181414.5		
			GCCCAAGTGGCCTTGACTAT	AGTCATGCATTCCTTGGCGA
<i>Vps15</i>	Phosphatidylinositol 3 kinase, regulatory subunit, polypeptide 4, p150	NM_001081309.1		
			TCATGCCGTATCTTGACCCG	TCTGAACAAGCTGGCGATGT
<i>Becn1</i>	Beclin 1, autophagy related	NM_019584.3	GCCTGGGCTGTGGTAAGTAA	CCAGCCTCTGAAACTGGACA
<i>Atg14</i>	Autophagy related 14	NM_172599.4	GAGCATAACAACCCCGCTA	CTTGCTGAGTTTTCCGCCAC
<i>Lc3a</i>	Microtubule-associated protein 1 light chain 3 alpha	NM_025735.3		
			TACATGGTCTACGCCTCCCA	GCCTAATCCACTGGGGACTG
<i>Lc3b</i>	Microtubule-associated protein 1 light chain 3 beta	NM_026160.4		
			GCTCGCTGCTGTCTAGATGT	CAGTCGCTTAAGCTGGGTCA
<i>Gabarap</i>	Gamma-aminobutyric acid receptor associated protein	NM_019749.4	GAAGCGAATTCATCTCCGTGC	CGCTTTCATCACTGTAGGCAA
<i>Gabarapl1</i>	Gamma-aminobutyric acid (GABA) A receptor-as- sociated protein-like 1	NM_020590.4	AGGACCACCCCTCGAGTAT	GGAGCCTTCTCCACGATGAC
<i>Gabarapl2</i>	Gamma-aminobutyric acid (GABA) A receptor-as- sociated protein-like 2	NM_026693.5	CTTCCGTCGCCATGAAGTG	AGCCCGAGACTTTTTCCACG
<i>Atg7</i>	Autophagy related 7	NM_001253717.1	GCTTCTGCCATGAGGCTT	TAAAGGGGGCGAACTGCAAC
<i>Atg3</i>	Autophagy related 3	NM_026402.3	GTGGCAGCTGGAGTCACTT	ACACCGCTGTAGCATGGAA
<i>Atg4a</i>	Autophagy related 4A, cysteine peptidase	NM_174875.3	GCCTTGGGATTTTCTGCAAAG	GGCTTGGCTGGAGGTACAAA
<i>Atg4b</i>	Autophagy related 4B, cysteine peptidase	NM_174874.3	CAGCACCCCTCCCTTAGGAT	CACCTCCAAGCTGGGATAGC
<i>Atg4c</i>	Autophagy related 4C, cysteine peptidase	NM_175029.3	TCTGCTTCTCTGAGGGTTA	TCTGTTCTGAAGCCTCCATA
<i>Atg4d</i>	Autophagy related 4D, cysteine peptidase	NM_153583.10	CTAGCAACCTGGGACCTTCG	CCGGCTTTTAACTGCCCAAC
<i>Atg12</i>	Autophagy related 12	NM_026217.3	GAGGAACCTCCGGAGACA	TTGCTCCACAGCCCATTTC
<i>Atg10</i>	Autophagy related 10	NM_025770.3	GCGAGCGGGTTCTCATTAAAC	TGCACATGTAGCCATCAGAACA
<i>Atg16l1</i>	Autophagy related 16-like 1	NM_001205391.1	GCAGCAAAGGAACCTCTACCT	AGGCTGCGAGAGTCGCTTA
<i>Atg5</i>	Autophagy related 5	NM_053069.5	CCAGTTTTGGCCATCAACC	CTTCTGGATGAAAGGCCGCT
<i>Bnip3</i>	BCL2/adenovirus E1B interacting protein 3	NM_009760.4	GGTCGACTTGACCAATCCCA	CCACAGCTTGGCGAGAAAA
<i>Bnip3l</i>	BCL2/adenovirus E1B interacting protein 3-like	NM_009761.3	GGCTTTTCGTCTCCCTCAGT	CCTTCTCATGTGCTGGCCT
<i>Dram1</i>	DNA-damage regulated autophagy modulator 1	NM_027878.2	ATGATCGATTGCAGGAGCGT	TTGGTGGGATGCATCGGAAT
<i>Npc1</i>	Niemann-Pick type C1	NM_008720.2	ACTGTTGGCAGTGTGGTGC	TTTCGGACACAGAAAGCCCC
<i>Vmp1</i>	Vacuole membrane protein 1	NM_029478.3	AAGTCACCATCTGCTCCACG	TGTGGGCACCTCTGTGACC
<i>Ambra1</i>	Autophagy/Beclin 1 regulator 1	NM_172669.3	AGGATCCAGAGAGCACCCAA	CGCTGGCGAATACTGTCTCT
<i>Irgm1</i>	immunity-related GTPase family M member 1	NM_008326.1	CATAGGGAACCTCTGCCGGA	AGTTGGTTCCTCGAATGCCT
<i>Rgs19</i>	Regulator of G-protein signaling 19	NM_001291205.1	GGACCTCCAGTCGCAATC	CTCGTTGCCGTTCTTGGTTC
<i>Mpz</i>	Myelin protein zero	NM_008623.4	CGGACAGGGAAATCTATGGTGC	TGGTAGCGCCAGGTAAAAGAG
<i>Mbp</i>	Myelin basic protein	NM_001025251.2	AATCGGCTCACAAAGGGATTCA	TCCTCCAGCTTAAAGATTTGG

Table S1. List of primers used for RT-qPCR (Continued)

Gene		Accession	Sense sequence (5'-3')	Antisense sequence (5'-3')
<i>Gapdh</i>	Glyceraldehyde-3-phosphate dehydrogenase	NM_001289726.1	TGCACCACCAACTGCTTAG	GGATGCAGGGATGATGTC
<i>Shh</i>	Sonic hedgehog	NM_009170.3	AAAGCTGACCCCTTAGCCTA	TTCGGAGTTTCTTGATCTTCC
<i>Olig1</i>	Oligodendrocyte transcription factor 1	NM_016968.4	CCGCCCCAGATGTACTATGC	AACCCACCAGCTCATA CAGC
<i>Gdnf</i>	Glial cell line derived neurotrophic factor	NM_010275.3	GATTCGGGCCACTTGGAGTT	GACAGCCACGACATCCCATA

Table S2 shows changes in levels of individual lipid species after nerve injury in ATG7 WT and cKO mice as determined by UPLC analysis of purified myelin and is provided as a Word file.